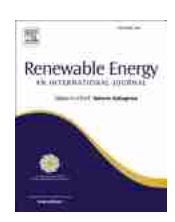
ELSEVIER

Contents lists available at ScienceDirect

Renewable Energy

journal homepage: www.elsevier.com/locate/renene





Adaptive management of borehole heat exchanger fields under transient groundwater flow conditions

Hesam Soltan Mohammadi*, Lisa Maria Ringel, Christoph Bott, Peter Bayer**

Department of Applied Geology, Institute of Geosciences and Geography, Martin Luther University Halle-Wittenberg, Von-Seckendorff-Platz 3, 06120, Halle (Saale), Germany

ARTICLE INFO

Keywords:
Heating and cooling
Uncertainty
Optimization
Groundwater flow
Borehole heat exchanger
Transient simulation

ABSTRACT

Uncontrolled heat extraction by multiple interacting borehole heat exchangers (BHEs) in high-density energy-use districts can lead to undesirable thermal conditions in the subsurface which can affect both system performance and regulatory compliance. The difficulty in controlling heat extraction arises in particular from predictive uncertainties, such as when forecasting trends in energy demand or groundwater flow. In this study, a combined simulation-calibration-optimization framework is introduced to consider BHE fields with the presence of a transient groundwater flow regime. In the first part, a semi-analytical modeling technique is proposed based on temporal superpositioning of variable flow conditions. Two synthetic case studies verify its accuracy under different groundwater fluctuation patterns. The mean absolute error of the proposed model in comparison to numerical calculation does not exceed 0.18 K over ten years of operation. In the second part, the model is augmented by a parameter estimation algorithm that is employed for continuous model updating. The benefit of resolving transient flow conditions is demonstrated by using this approach for monthly optimization of individual BHE heat extraction. The result of dynamic optimization compared to a synthetic case without calibration shows a 10 % lower imposed temperature change in the subsurface.

Nomenclature

С	Specific heat capacity (Jkg ⁻¹ K ⁻¹)	
\overrightarrow{e}	All-ones vector	
H	Characteristic length (m)	
k	Counter index for the number of BHEs	
1	Counter index for the number of time steps	
L	Length of borehole (m)	
m	Counter index for optimization time steps	
n	Porosity (–)	
N_{BHE}	Number of BHEs	
N_t	Number of time steps	
N_{topt}	Number of optimization time steps	
q	Heat extraction/injection rate (Wm ⁻¹)	
r	Horizontal distance to the BHE axis (m)	
S	Field domain	
t	Time (s)	
T	Temperature (K)	
и	Specific discharge (ms ⁻¹)	
ν_a	Seepage velocity (ms ⁻¹)	
vhc	Volumetric heat capacity (Jm ⁻³ K ⁻¹)	
	(continued on next column)	

(continued)

w	Weighting factor (–)	
x	Coordinate in x-direction (m)	
y	Coordinate in y-direction (m)	
Z	Coordinate in z-direction (m)	
#	Auxiliary variable	
α	Thermal diffusivity (m ⁻² s ⁻¹)	
ΔT	Temperature change (K)	
λ	Thermal conductivity (Wm ⁻¹ K ⁻¹)	
ρ	Density (kg m ⁻³)	
v_T	Heat transport velocity (ms ⁻¹)	
ω	Thermal response coefficient (-)	
Subscripts for material properties		
m	Medium	
s	Solid	
w	Water	

1. Introduction

In recent decades, shallow geothermal systems have arisen as a promising solution for meeting energy needs in the heating and cooling

E-mail addresses: hesam.soltan-mohammadi@geo.uni-halle.de (H. Soltan Mohammadi), peter.bayer@geo.uni-halle.de (P. Bayer).

https://doi.org/10.1016/j.renene.2024.121060

Received 26 March 2024; Received in revised form 5 June 2024; Accepted 22 July 2024 Available online 22 July 2024

^{*} Corresponding author.

^{**} Corresponding author.

of buildings [1]. Interest in these systems is driven by the pursuit of an energy transition and the impetus to reduce carbon emissions. Due to the relatively constant temperatures of the ground, sustainable heating and cooling is achieved by extracting and injecting heat through a heat carrier fluid within borehole heat exchangers (BHEs) coupled with ground source heat pumps (GSHP) [2]. Even though BHEs are the cornerstone of shallow geothermal systems, their optimal performance depends on various factors, including the often overlooked dynamic hydrogeological conditions of the subsurface. Beyond considering engineering and mechanical aspects, a detailed insight into the thermal properties of the subsurface is crucial for the reliable design of these systems. To this end, thermal response tests (TRTs) are the standard procedure to thermally characterize the subsurface that is the target for installation of single or multiple BHE fields. Here, a controlled thermal load is imposed and the subsequent temperature response of the subsurface is measured [3,4]. The main limitation of TRTs is their short-term nature and they are mainly carried out during the design phase. While TRTs provide valuable initial characteristics of a field including groundwater flow (GWF) effects, they cannot capture the long-term transient behavior of the subsurface thermal regime. This is due to dynamic factors and uncertainties such as seasonal variations [5], long-term climatic changes [6], heterogeneity [7–11], and transient hydrogeological conditions of the subsurface [12], which can profoundly affect the performance of operating BHE fields in practice [13,

The role of hydrogeological conditions in a field with operating BHEs has been examined in various studies as they affect the governing heat transfer mechanism in the subsurface [15,16]. For example, Ma et al. [17], in a system of BHEs coupled with pumping-injection well, investigated the role of groundwater-forced seepage on the thermal performance of BHEs. The impact of tidal-induced GWF on the heat exchange rate of a BHE was evaluated by Moreira et al. [18]. He et al. [19], by creating a numerical model in combination with a physical sandbox experiment, studied various BHE configurations to optimize the operation in the presence of GWF. Deng et al. [20] investigated the consideration of thermal imbalance in BHEs during operating periods in areas with strong seasonal groundwater fluctuations. The underlying rationale was that the accumulated heat can be balanced by the use of groundwater heat in the other seasons, thus achieving a year-round thermal balance. In a laboratory seepage box supported by a numerical model, Li et al. [21] attempted to determine the role of GWF on the heat exchange of a BHE in a layered geological setting with saturated and unsaturated

Most studies focused on investigating the role of GWF in the performance of BHEs. This emphasis stems from the constraints imposed by economic considerations and legislation, as significant changes in subsurface thermal conditions of groundwater bodies are often restricted [22,23]. As the thermal processes in the subsurface are generally gradual and slow, uncontrolled energy extraction can lead to irreversible and potentially critical thermal anomalies. Short-term thermal imbalances directly affect the performance of heat pumps, while rectifying these anomalies in the long term poses a significant hurdle and can lead to environmental and technical complications that may call into question the feasibility of continued operation. As a remedy, various optimization methods have been developed to systemically distribute the heating/cooling demand among individual BHEs in a field. Beck et al. [24,25] pioneered mathematical optimization of BHE fields, aiming to minimize temperature anomalies by tuning individual loads, thus addressing both ecological and economic concerns. Bayer et al. [26] followed the same optimization concept and suggested identifying inefficient BHEs and decommissioning them to enhance the overall performance of the field. In further work, Hecht-Mendez et al. [27] integrated GWF into the combined simulation-optimization framework.

Aside from these earlier works, multiple efforts were undertaken to mathematically fine-tune the spacing, placement, length, and number of BHEs in fields with fixed energy demand [28–32]. However, these optimization procedures primarily target minimizing capital costs and achieving economic efficiency by optimizing the design parameters and not the operational parameters. These procedures rely entirely on deterministic models in a commonly static manner. Static means that the modeling tool does not take into account naturally variable or uncertain future thermal states of the ground and optimal solutions are fully based on the initial prediction. However, the thermal evolution in the subsurface for several decades, given the wide array of complexities in the ground, and the ramifications of initial uncertainties, can hardly be predicted.

To increase the applicability of optimization algorithms for realworld cases, it is advantageous to use dynamic optimal control strategies. The underlying idea of most optimal control strategies is centered on model simulation and retrieving feedback from the real system in a given time horizon [33,34]. In these algorithms, by monitoring measurements and using the deviation between the measurements and the simulations, the model input parameters are adjusted and consequently, new optimized parameters are provided [35-37]. Although advanced control algorithms have been employed for geothermal systems [38-40], the applied predictive models are highly simplified and typically cannot accurately reproduce the thermal dynamics of the subsurface [41]. For instance, Soltan Mohammadi et al. [42,43] extended the optimization of load balancing in a BHE field in a sequential fashion to account for subsurface and energy demand uncertainties. However, advective heat transfer was not considered, the model parameters were not calibrated, and the uncertainty in the subsurface thermal response was not addressed from a physics-based perspective.

To make this approach more robust, the novel strategy in this work is to revisit the optimization process systematically at a certain frequency, and to update the proposals for the next months' load patterns by calibrating the model parameter based on the measured thermal history of the field. However, the frequency of model calibration can differ from the temporal resolution of the optimal load proposals. In this study, the learning potential of iterative simulation-optimization for management of a BHE field with transient hydrogeological conditions during the operation is investigated. The general proposed approach is to reperform the optimization after a certain period of operation, here on a monthly basis, and to take the measured thermal state of the ground as the new initial condition for the simulation of the upcoming months. By sequentially minimizing the maximum temperature variations arising from the operation of the BHEs, it is intended to impede local decline of the underground temperatures. The key idea is to mitigate extreme cooling by switching the allocated energy demand from the most critical BHEs to the ones that are theoretically less prone to local cool-downs based on the simulated results of a predictive model.

For testing and demonstration, we investigate scenarios in which the subsurface thermal conditions change due to the natural dynamics of GWF. For this, in Section 2.1 the moving finite line source (MFLS) is formulated to include transient GWF conditions. All details about the integration of this model in a sequential optimization-calibration process are described in Section 2.2. The configuration of the BHEs, the model parameters, and the groundwater fluctuation patterns in different scenarios are presented in Section 2.3. In Sections 3.1 and 3.2, numerical models are developed and employed to verify the accuracy of the proposed formulation of the analytical model for a single BHE and a BHE field, respectively. The results of optimized load patterns for the BHE field and the calibration are presented in Section 3.3. Section 4 concludes the current work with an outlook on future studies.

2. Methodology

2.1. Simulation of a borehole heat exchanger field

The spatial and temporal evolution of the temperature distribution in the subsurface due to the operation of a BHE system in an aquifer can be estimated by a semi-analytical solution, the so-called moving finite line-source (MFLS) model [44,45]:

load as a series of $l=1,...,N_t$ load pulses $\overrightarrow{q}=\left(q_{1,1},...,q_{N_{BHE},1},...,q_{1,N_t},...,q_{N_{BHE},N_t}\right)^T$ for each borehole and each time step, and a velocity $v_{T,l}$, that changes in each time step l [24,27]. This results in determining the temperature variation at any given location relative to a borehole, denoted as x_i, y_j , and at a specific time t:

$$\Delta T(q, x, y, z, t) = \frac{q}{2\pi\lambda} \exp\left(\frac{v_T x}{2\alpha}\right) \left(\int_0^L \frac{1}{4r} \left(\exp\left(\frac{-v_T r}{2\alpha}\right) \operatorname{erfc}\left(\frac{r - v_T t}{2\sqrt{\alpha t}}\right) + \exp\left(\frac{v_T r}{2\alpha}\right) \operatorname{erfc}\left(\frac{r + v_T t}{2\sqrt{\alpha t}}\right)\right) dz'$$

$$-\int_{-L}^0 \frac{1}{4r} \left(\exp\left(\frac{-v_T r}{2\alpha}\right) \operatorname{erfc}\left(\frac{r - v_T t}{2\sqrt{\alpha t}}\right) + \exp\left(\frac{v_T r}{2\alpha}\right) \operatorname{erfc}\left(\frac{r + v_T t}{2\sqrt{\alpha t}}\right)\right) dz'$$
(1)

This assumes that heat is distributed through both conduction and advection via GWF in a homogeneous subsurface with an isotropic thermal conductivity. The properties of the porous media do not depend on the temperature. Further assumptions are that the subsurface is initially at thermal equilibrium conditions, that the surface temperature

$$\overrightarrow{\Delta T} \left(\overrightarrow{q}, x_i, y_j, z, t \right) = \sum_{l=1}^{NL} \sum_{k=1}^{N_{BHE}} q_{k,l} \omega_{k,l} \left(x_i, y_j, z, t \right) \tag{7}$$

with the response coefficient:

$$\begin{split} &\omega_{k,l}\left(x_{l},y_{j},z,t,\upsilon_{T,l}\right) = \frac{1}{2\pi\lambda}\exp\left(\frac{\upsilon_{T,l-1}x}{2\alpha}\right)\left(\int_{0}^{L}\frac{1}{4r}\left(\exp\left(\frac{-\upsilon_{T,l-1}r}{2\alpha}\right)\operatorname{erfc}\left(\frac{r-\upsilon_{T,l-1}\Delta t_{l-1}}{2\sqrt{\alpha\Delta t_{l-1}}}\right) + \exp\left(\frac{\upsilon_{T,l-1}x}{2\alpha}\right)\operatorname{erfc}\left(\frac{r+\upsilon_{T,l-1}\Delta t_{l-1}}{2\sqrt{\alpha\Delta t_{l-1}}}\right)\right)dz'\\ &-\int_{-L}^{0}\frac{1}{4r}\left(\exp\left(\frac{-\upsilon_{T,l-1}r}{2\alpha}\right)\operatorname{erfc}\left(\frac{r-\upsilon_{T,l-1}\Delta t_{l-1}}{2\sqrt{\alpha\Delta t_{l-1}}}\right) + \exp\left(\frac{\upsilon_{T,l-1}r}{2\alpha}\right)\operatorname{erfc}\left(\frac{r+\upsilon_{T,l-1}\Delta t_{l-1}}{2\sqrt{\alpha\Delta t_{l-1}}}\right)\right)dz'\\ &-\int_{0}^{L}\frac{1}{4r}\left(\exp\left(\frac{-\upsilon_{T,l}r}{2\alpha}\right)\operatorname{erfc}\left(\frac{r-\upsilon_{T,l}\Delta t_{l}}{2\sqrt{\alpha\Delta t_{l}}}\right) + \exp\left(\frac{\upsilon_{T,l}r}{2\alpha}\right)\operatorname{erfc}\left(\frac{r+\upsilon_{T,l}\Delta t_{l}}{2\sqrt{\alpha\Delta t_{l}}}\right)\right)dz' + \int_{-L}^{0}\frac{1}{4r}\left(\exp\left(\frac{-\upsilon_{T,l}r}{2\alpha}\right)\operatorname{erfc}\left(\frac{r-\upsilon_{T,l}\Delta t_{l}}{2\sqrt{\alpha\Delta t_{l}}}\right) + \exp\left(\frac{\upsilon_{T,l}r}{2\alpha\Delta t_{l}}\right)\right)dz'\right), \end{split}$$

is constant, and that the heat is extracted at a constant rate over the BHE length. In Equation (1), $\Delta T = T_\infty - T$ refers to the temperature change with regard to the undisturbed temperature T_∞ . L denotes the borehole length, λ is the thermal conductivity, α is the thermal diffusivity, and r signifies the distance to the BHE axis $x,\,y,$ and the vertical axis of a borehole (z-z'), calculated as $r=\sqrt{x^2+y^2+(z-z')^2}$. It is important to emphasize that the MFLS solution provides temperature at specific distance and depth, denoted by r and z, respectively, and should not be regarded as a fully resolved 3D solution. q stands for the heat injection/extraction per length of the BHE, with a positive value indicating heat extraction, u is the specific discharge, v_a is the seepage velocity and v_T is the effective heat transport velocity determined by the following equations:

$$vhc_s = c_s \rho_s \tag{2}$$

$$vhc_{w} = c_{w}\rho_{w} \tag{3}$$

$$vhc_m = (1 - n) \times vhc_s + n \times vhc_w \tag{4}$$

$$v_a = u/n \tag{5}$$

$$v_T = v_a \times n \times vhc_w/vhc_m \tag{6}$$

The superposition principle can be applied to account for a set of boreholes $k=1,...,N_{BHE}$ at locations (x_k,y_k) , a temporal variation of the

In Equations (7) and (8), the time steps are calculated as $\Delta t_{l-1} = t - t_{l-1}$ and $\Delta t_l = t - t_l$, where t is the current time $t \ge t_l$ [24–26,46–48]. Due to the assumption of temperature-independent parameters, the temperature distribution can be formulated as a linear problem according to:

$$\overrightarrow{\Delta T} \left(\overrightarrow{q}, x_i, y_j, t, v_{T,l} \right) = \overrightarrow{\omega} \left(x_i, y_j, t, v_{T,l} \right) \overrightarrow{q}$$
(9)

with $\overrightarrow{\omega} = (\omega_{1,1},...,\omega_{N_{BHE},1},...,\omega_{1,N_t},...,\omega_{N_{BHE},N_t})$. As an initial condition, $\overrightarrow{\Delta T} \left(\overrightarrow{q}, x_i, y_j, t_0 \right) = 0$ holds for $t_0 = 0$.

Due to the simplifying assumptions of MFLS, the absolute temperatures simulated by this model may not fully represent the exact thermal conditions in the subsurface [49]. However, it can approximate the relative thermal states around BHEs accurately [16,50]. Since the proposed optimization approach does not depend on absolute temperature simulations, MFLS is used as a fast proxy to estimate the effects of groundwater flow in a field with multiple active BHEs. This allows for assessing the contribution of each BHE in providing the heating/cooling demands in an iterative optimization framework.

2.2. Optimization-calibration procedure

The underlying optimization strategy is derived from the approach originally developed by de Paly et al. [46]. Mathematically, the proposed approach involves determining the position of the BHE within a field domain $x_i, y_j \in S$ at which the highest temperature change occurs.

Based on this, it reallocates the loads temporally and spatially to the other available BHEs in order to minimize the weighted sum of the maximum temperature changes over the operating time and the individual time steps:

$$\operatorname{argmin}\left(w \cdot \max\left(\overrightarrow{\Delta T}\left(\overrightarrow{q}, x_i, y_j, t_{N_t}\right)\right) + \sum_{l=1}^{N_t} \max\left(\overrightarrow{\Delta T}\left(\overrightarrow{q}, x_i, y_j, t_l\right)\right)\right),\tag{10}$$

subject to the constraints:

$$E_l = \sum_{k=1}^{N_{BHE}} q_{k,l}\,, \ egin{aligned} oldsymbol{x}_i, oldsymbol{y}_j \in S, \end{aligned}$$

for all $l=1,\ldots,N_t$. Within the optimization framework, this constraint serves as an essential criterion, ensuring the consistent fulfillment of energy demands across all time steps. In Equation (10), priority is given to the primary term to minimize temperature variance across the entire temporal spectrum by applying a weighting factor of w=100. The original concept of tuning BHE loads is to divide the operating time into l discrete intervals and derive an optimal transient heat load distribution based solely on the initial conditions at time t_0 (before the BHE field is operated), which hereafter is referred to as "single-step optimization". This approach can only propose optimal patterns at the design stage based on the initial thermal conditions of a field.

To enable a computationally efficient solution, the previously defined objective function (Equation 10) is revised to facilitate posing and solving the optimization problem as a linear one. This is accomplished by introducing virtual auxiliary variables ε_0 and ε_1 .

$$\min\left(\boldsymbol{w}\cdot\boldsymbol{z}_0+\sum_{l=1}^{Nt}\boldsymbol{z}_l\right),\tag{12}$$

subject to the constraints

$$\overrightarrow{\Delta T}\left(\overrightarrow{q}, x_{i}, y_{j}, t_{N_{t}}\right) - \varepsilon_{0} \overrightarrow{e} < 0,$$

$$-\overrightarrow{\Delta T}\left(\overrightarrow{q}, x_{i}, y_{j}, t_{N_{t}}\right) - \varepsilon_{0} \overrightarrow{e} < 0,$$

$$\overrightarrow{\Delta T}\left(\overrightarrow{q}, x_{i}, y_{j}, t_{l}\right) - \varepsilon_{l} \overrightarrow{e} < 0,$$

$$-\overrightarrow{\Delta T}\left(\overrightarrow{q}, x_{i}, y_{j}, t_{l}\right) - \varepsilon_{l} \overrightarrow{e} < 0,$$

$$E_{l} = \sum_{k=1}^{N_{BHE}} q_{k,l},$$

$$x_{l}, y_{j} \in S,$$
(13)

for all $l = 1, ..., N_t$. \overrightarrow{e} denotes the vector of ones with N_{BHE} entries.

In the adaptive strategy, monthly deviations between the simulated and measured temperatures form the basis for a new optimization and the allocation of the new load patterns for the following months. The adaptive optimization process is conducted iteratively over predefined time intervals t_m ($m=1,...,N_{topt}$). $\overrightarrow{\Delta T}_{meas}\left(x_i,y_j,t_{m-1}\right)$ is considered as the real-time monitored data in the field, and $\overrightarrow{\Delta T}\left(\overrightarrow{q},x_i,y_j,t_{m-1}\right)$ is the output of simulations based on the proposed MFLS model. Taking into account the monthly measured temperature as an indicator of the actual thermal conditions of the subsurface, a revised optimal load pattern, \overrightarrow{q} , is computed for the individual BHEs at each time step. This approach is implemented as an iterative loop for $m=1,...,N_{topt}$:

$$\min\left(z_0 + \sum_{l=m}^{Nt} w_{l}z_l\right),\tag{14}$$

subject to the constraints:

$$\overrightarrow{\Delta T} \left(\overrightarrow{q}, x_{i}, y_{j}, t_{N_{t}} \right) - \overrightarrow{\Delta T} \left(\overrightarrow{q}, x_{i}, y_{j}, t_{m-1} \right) - \varepsilon_{0} \overrightarrow{e} < - \overrightarrow{\Delta T}_{meas} \left(x_{i}, y_{j}, t_{m-1} \right), \\
- \overrightarrow{\Delta T} \left(\overrightarrow{q}, x_{i}, y_{j}, t_{N_{t}} \right) + \overrightarrow{\Delta T} \left(\overrightarrow{q}, x_{i}, y_{j}, t_{m-1} \right) - \varepsilon_{0} \overrightarrow{e} < \overrightarrow{\Delta T}_{meas} \left(x_{i}, y_{j}, t_{m-1} \right), \\
\overrightarrow{\Delta T} \left(\overrightarrow{q}, x_{i}, y_{j}, t_{l} \right) - \overrightarrow{\Delta T} \left(\overrightarrow{q}, x_{i}, y_{j}, t_{m-1} \right) - w_{l} \varepsilon_{l} \overrightarrow{e} < - \overrightarrow{\Delta T}_{meas} \left(x_{i}, y_{j}, t_{m-1} \right), \\
- \overrightarrow{\Delta T} \left(\overrightarrow{q}, x_{i}, y_{j}, t_{l} \right) + \overrightarrow{\Delta T} \left(\overrightarrow{q}, x_{i}, y_{j}, t_{m-1} \right) - w_{l} \varepsilon_{l} \overrightarrow{e} < \overrightarrow{\Delta T}_{meas} \left(x_{i}, y_{j}, t_{m-1} \right), \\
E_{l} = \sum_{k=1}^{N_{BHE}} q_{k,l}, \\
x_{l}, y_{j} \in S, \tag{15}$$

for all $l=m,...,N_t$. In this iterative process, the simulated temperatures are replaced by the measured temperatures, when they become available.

As a further modification, the first term of the objective function is divided into two separate time windows: a short-term horizon (upcoming 12 months) with higher significance ($w_l = 100$) and a long-term horizon (remaining time until the end of the operational lifetime) with lower significance ($w_l = 1$). Since the proposed optimization is an iterative process, at some point all time steps will be considered as short-time horizons with higher impact. The rationale for this is that due to different and mostly unpredictable uncertainties in long-time horizons, e.g., a few decades, it is better to consider the next year as the short-time horizon, which merits a higher weight since its predictability is better.

In addition, the assumed model parameters will be updated simultaneously based on the measured data from all previous time steps. This enables the algorithm not only to initiate the optimization from a correct thermal state but also to learn about the evolution of time-varying parameters that could be the cause of the deviations between the measurements and the simulations, thereby avoiding accumulation of errors. This proposed simulation-optimization-calibration procedure is referred to hereafter as "sequential optimization".

To consider the effects of GWF on optimal BHE load patterns and system performance, this study assumes that the only model parameter that varies is the GWF velocity. Therefore, in the example cases, unknown GWF evolution during the course of BHE field operation is the only cause of uncertainty in the subsurface temperatures. To calibrate the GWF velocity, the problem is mathematically formulated as nonlinear least squares minimization. The discrepancy between the measured and simulated temperature is considered as an argument for the objective function. The Trust-Region-Reflective algorithm, implemented in MATLAB as an optimization technique, is employed to solve this problem. In this method, the optimization variables are iteratively adjusted within a trust region, i.e., a local region around the current solution. This algorithm effectively balances local and global information to navigate efficiently through the optimization domain, making it robust for dealing with nonlinear constraints and boundary conditions on the optimization variables. By adaptively updating the size of the confidence region and the model parameter, the algorithm converges to a local minimum of the objective function and provides a solution to the parameter estimation problem [51].

In the proposed adaptive framework, the temporal resolution of calibration and optimization does not necessarily have to be identical. However, in this work, it is assumed that at the end of each month, the optimal load patterns are modified and proposed for the remaining months. Since it is presumed that monitoring takes place at the end of each month as well, the model is also calibrated on a monthly basis. Therefore, in this study, both the iteration of the optimization and the calibration have a length of one month. To start the optimization, the initial estimate of GWF velocity is assumed to be correct for the first

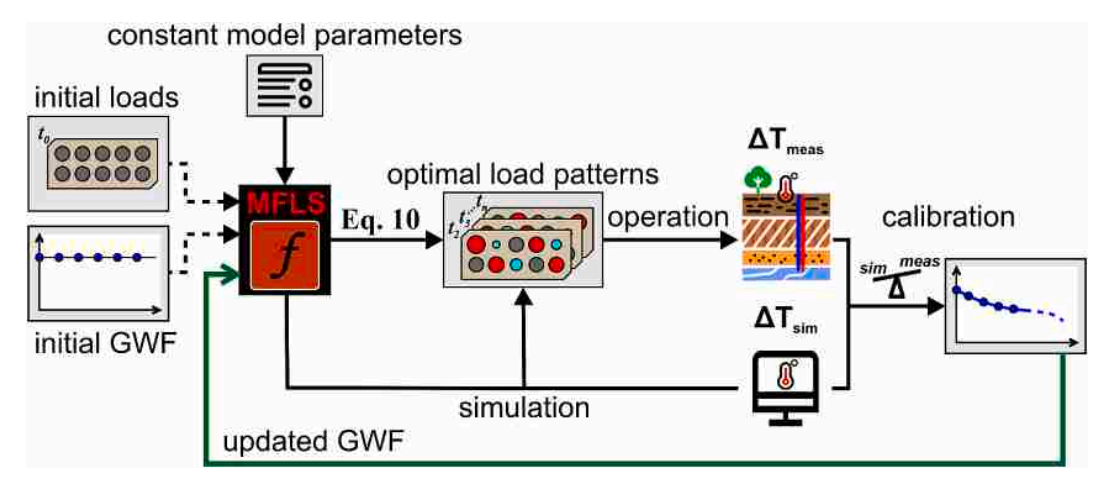


Fig. 1. Conceptual flowchart of the proposed adaptive optimization of individual loads for BHEs in a field.

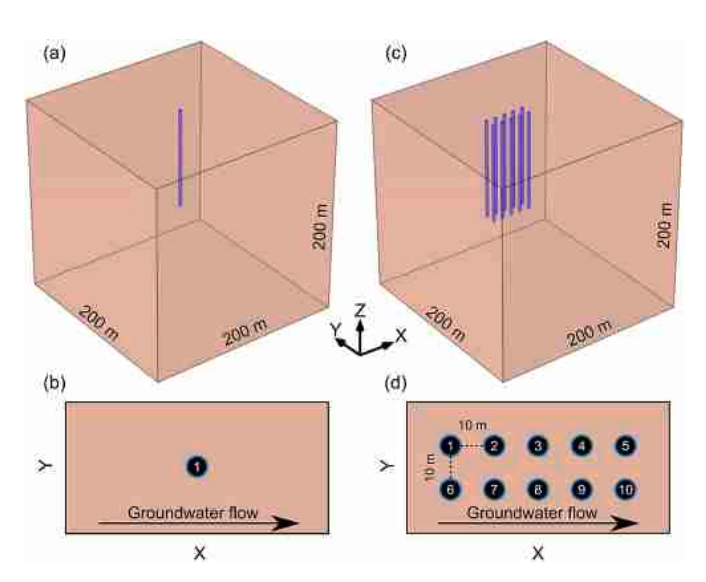


Fig. 2. Spatial 3D layout of a field with (a) one BHE and (c) multiple BHEs. Subplots (b) and (d) depict groundwater flow direction and the top view of the field with one BHE and multiple BHEs, respectively.

month based on the site characterization measurements before the field is commissioned. From the second month onwards, once no more true information is available to revise the model parameters, model calibration makes sense. In calibration calculations, the previous month's GWF velocity is used as the initial guess. This serves as the best rough estimate. By minimizing the calibration function, a new GWF is determined and used as the input for the simulation and optimal proposals of the next months. The flowchart of the proposed method is shown in Fig. 1.

Table 1Parameter specifications for case studies.

Parameter	Value	Unit
Length of borehole, L	100	m
Thermal conductivity, λ	2.42	${ m W} { m m}^{-1} { m K}^{-1}$
Thermal diffusivity, α	4.32×10^{-7}	$m^2 s^{-1}$
Specific heat capacity of solid, c_s	1920	$\rm J \ kg^{-1} K^{-1}$
Specific heat capacity of water, c_w	4192	$\rm J \ kg^{-1} K^{-1}$
Volumetric heat capacity, vhc	4819200	${ m J} \ { m m}^{-3} \ { m K}^{-1}$
Solid density, ρ_s	2650	$kg m^{-3}$
Fluid density (at 15 °C), ρ_w	1000	kg m ^{−3}
Porosity, n	0.30	_

2.3. Model set-up

In this study, two scenarios of BHEs are considered; one is a single BHE, and the other is an array of ten BHEs with a spacing of 10 m. As depicted in Fig. 2a and c, the BHEs are located in an area with a length of 200 m in each direction to reduce the influence of the model domain and boundary conditions on the results. Apart from conductive heat transfer, advective heat transport due to GWF also contributes to the evolution of the thermal regime of the subsurface. Therefore, it is required to consider a distance of 10 m between the BHEs in order not to violate any of the underlying thermal equilibrium assumptions of the MFLS model and to avert extreme thermal influences of neighboring BHEs [27,52]. Fig. 2b and d illustrate the GFW direction as well as the top view of the lattice arrangement of the BHEs. Here, BHE numbers are also introduced, which will be used in the following to refer to each particular BHE. All required materials and physical properties of the subsurface and the BHEs used for the MFLS and numerical models are given in Table 1.

For each BHE configuration, a monthly heating demand profile for the considered BHE fields is presented in Fig. 3. This pattern is repeated for ten years of operation. The presented energy demand is estimated for a BHE field with an annual operational duration of 1800 h. We assume a specific heat extraction rate of $50~\rm Wm^{-1}$ with a monthly distribution for

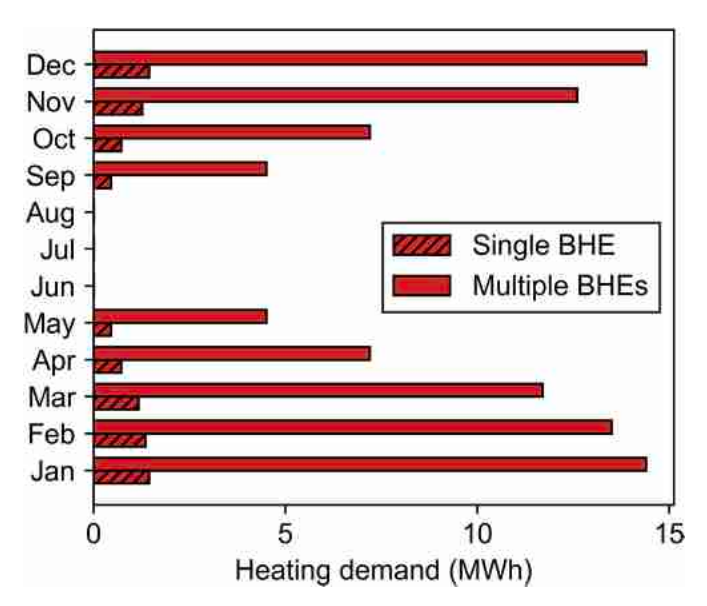


Fig. 3. Monthly heat demand profile for both BHE fields.

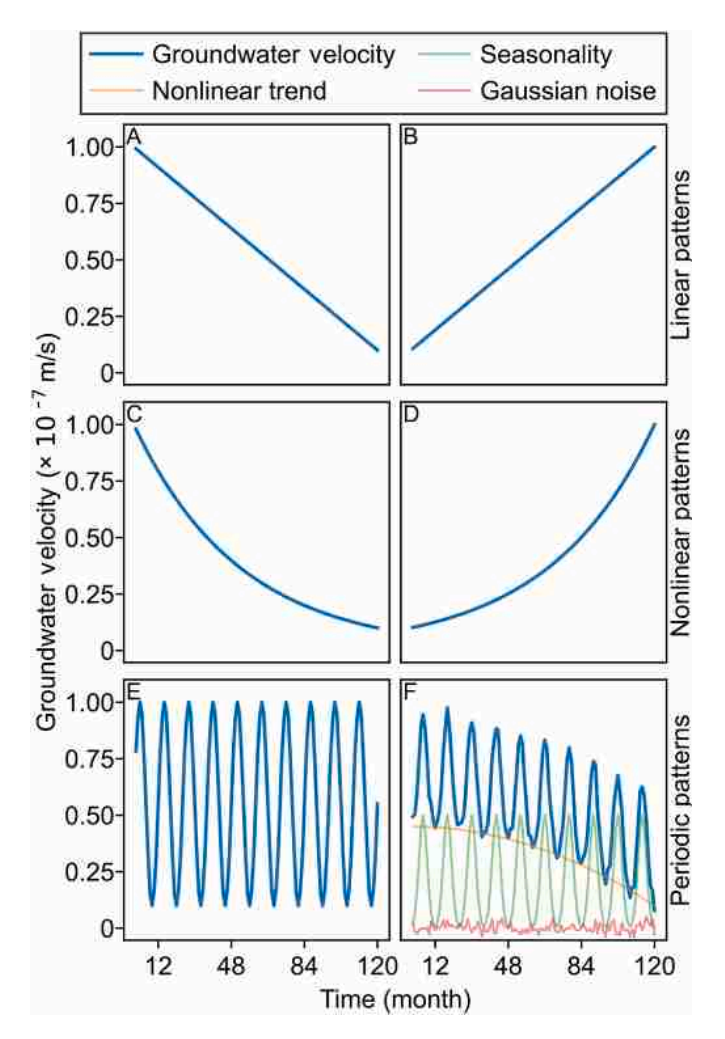


Fig. 4. Fluctuation in groundwater velocity over the ten years of operation with (A) linearly decreasing, (B) linearly increasing, (C) non-linearly decreasing, (D) non-linearly increasing, (E) periodic, and (F) periodically decreasing pattern. Pattern (F) is the overlay of a nonlinear decreasing trend, a periodic pattern, and a random noise.

a field located in a site with Central European weather conditions, only with heating application, and no energy demand in summer months. In the considered scenario with multiple BHEs, the operation takes place in parallel and each BHE is individually controllable.

To evaluate the impact of GWF, six different theoretical transient GWF fluctuation patterns with monthly resolution are considered. Different evolution patterns, including linear, nonlinear, and periodic with increasing, decreasing, or noisy trends, are introduced to validate the proposed rearrangement of the MFLS model (Equation 8). This includes transient GWF. All GWF patterns vary from 1×10^{-8} to $1\times 10^{-7}~\rm ms^{-1}$, and they are presented in Fig. 4. In order to characterize the relative dominance of advection to diffusion in the transport of heat in the field, the Péclet number is defined as:

$$P\acute{e} = \frac{v_a \rho_w c_w H}{\lambda} \tag{16}$$

where the spacing of the BHEs is considered as the characteristic length (H). The Péclet number varies in the range of 0.58–5.78, which represents groundwater flow velocities from low to high. These Péclet numbers indicate a broad range of heat transfer mechanisms, from scenarios where conduction dominates over advection (Pé < 1) to those where advection is the dominant heat transfer mechanism (Pé > 1). To evaluate transient heat transfer in the field, the Fourier number is

calculated as:

$$Fo = \frac{\alpha t}{H^2} \tag{17}$$

The Fourier number for a characteristic time of ten years results in a value of 1.36.

3. Results and discussion

3.1. Single borehole heat exchanger

This section investigates the accuracy of heat transfer simulations using the proposed rearrangement of MFLS (Equations 7, 8 and 9). To validate the results obtained from this semi-analytical solution, a numerical model is employed. The numerical model is implemented using the COMSOL Multiphysics software. Temperature changes are simulated over ten years, recording the temperature change with a monthly resolution, based on the monthly energy demand profile presented in Fig. 3. Temperature changes are recorded at four measurement locations (north, east, west, and south) around the BHE with a distance of 0.5 m from the BHE, at a depth of 50 m. The top surface of the numerical model has a fixed temperature boundary condition, and all other model boundaries are thermally insulated. A fixed temperature is applied

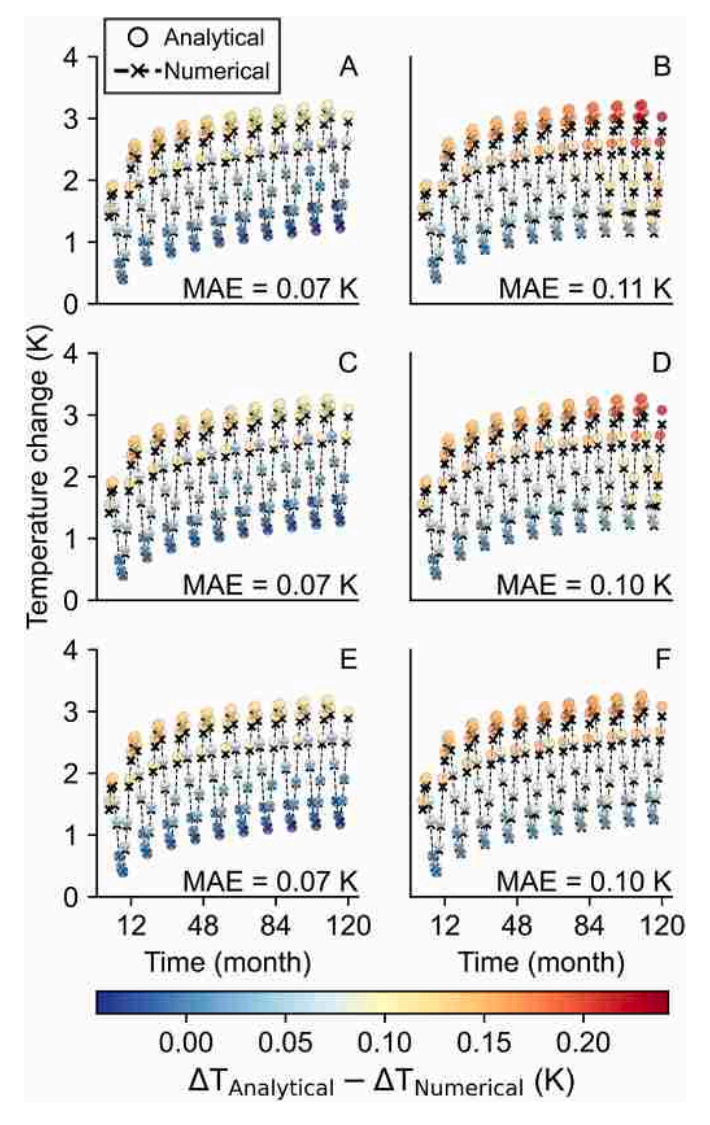


Fig. 5. Single BHE temperature obtained at a depth of 50 m for the ground-water flow patterns A–F (see Fig. 4).

throughout the domain as the initial undisturbed ground temperature for the model. The numerical model is carefully examined to ensure that the domain is sufficiently large, preventing any undesired effects from the boundaries due to thermal isolation. The BHEs are implemented as line heat sources with constant heat extraction rates along their lengths. To ensure the robustness of the approach, the temperature variations under the six different GWF scenarios of Fig. 4 are considered. Fig. 5 illustrates the resulting temperature evolution corresponding to each GWF pattern (A-F) over time. The color-coded circles in the figures indicate the error between the results obtained from the semi-analytical and numerical models. Further, the mean absolute error (MAE) of temperature change is reported for each hydrogeological scenario. The accuracy of the proposed formulation for a single BHE case among all six GWF patterns is substantiated by an acceptable error level and the replicated temperature trend, which mimics the trend of the numerical results. Across all scenarios, the MAE is between 0.07 and 0.11 K. Comparing patterns A-D indicates that decreasing GWF velocities lead to a slightly lower error level than the increasing patterns, which can be attributed to slower heat propagation with decreasing thermal gradients. This is consistent with the initial thermal equilibrium assumptions made during the development of the semi-analytical model. Simultaneously, more fluctuating patterns (case E and F) still show a good agreement between the semi-analytical and numerical models. The magnitude of the error for this case is in the range of the measurement error of standard monitoring devices and therefore considered acceptable in practice.

3.2. Multiple borehole heat exchangers

In the previous section, the applicability and accuracy of the rearranged MFLS model are validated against a numerical model for a single BHE. However, since the optimization of BHE fields is the ultimate goal of this study, the applicability of the proposed semi-analytical formulation in an operational field with multiple BHEs needs to be verified. For this purpose, a field with ten BHEs in operation with the layout as shown in Fig. 2 is considered. To investigate the effects of transient GWF, patterns C and F are selected for this case study (Fig. 4). Pattern C is chosen because its nonlinear decreasing trend of GWF highlights the importance of optimization-calibration. Without model parameter estimation, the high GWF velocity at the beginning is considered for the entire operational period. Therefore, local cooling is expected to be naturally mitigated by the high-velocity heat transport, reducing the need for optimization. However, if the hydrogeological regime changes such that the GWF decreases, the incorrect proposed load patterns can cause local thermal anomalies, if this information is not incorporated into the model. Furthermore, Pattern F is also chosen since it exhibits random fluctuations in addition to the decreasing tendency, which further complicates the simulation.

A similar numerical model is employed to serve as a reference and the accuracy of the temperature changes simulated with the MFLS model is compared with it. The boundary conditions of the numerical model are the same as those in the case of the single BHE. The temperatures are compared at a depth of 50 m and at four points evenly distributed around all individual BHEs at a distance of 0.5 m. As this is a symmetrical case, Fig. 6 only shows the temperature development of BHE #1, #3, and #5 for both the numerical and the semi-analytical model over ten years of operation. Similarly, the color within the circles corresponds to the discrepancy between the two models. It should be noted that the maximum MAE is slightly higher for the case with multiple BHEs compared to a single BHE. Fig. 5 shows the MAE for the whole system under six different GWF patterns, while Fig. 6 indicates the MAE at the position of three BHEs and only for GWF patterns C and F. Therefore, the MAE values in these figures should be carefully compared. To better assess the error in each case study, the range of error for the case with one BHE is reported as 0.29 K, whereas for multiple BHES, this is 0.56 K. Despite the higher level of error, the results of the semi-analytical model

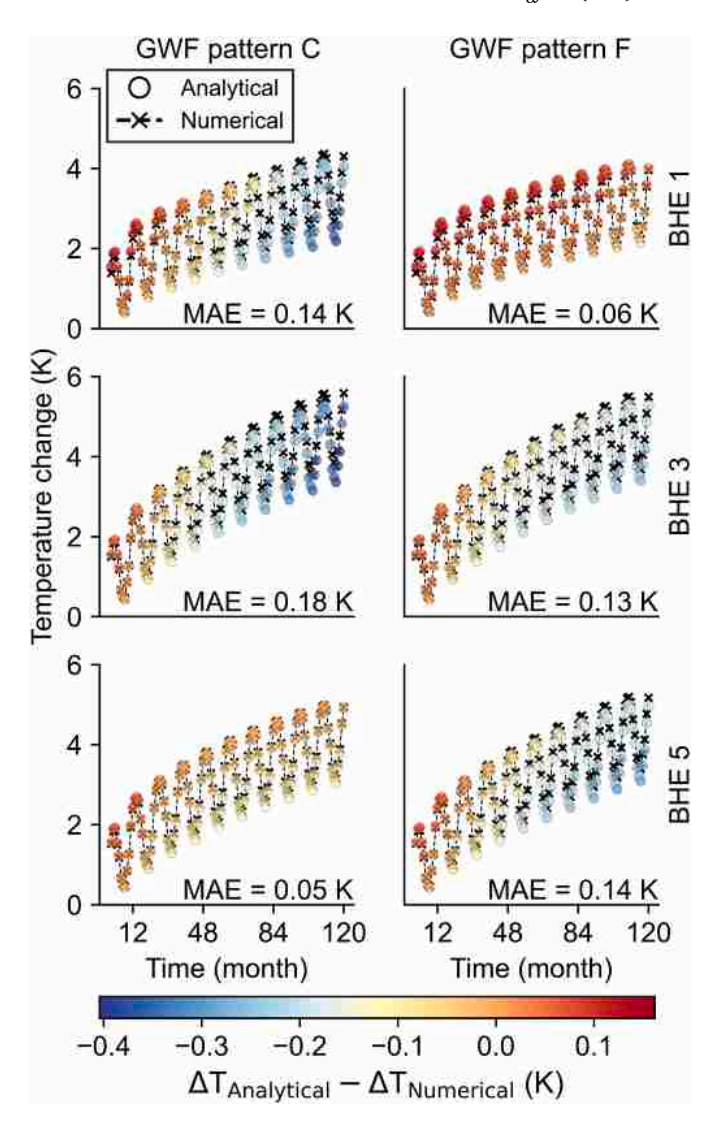


Fig. 6. Temperature change profile (analytical vs. numerical) for BHEs #1, #3, and #5 of the considered BHE field for groundwater flow velocity pattern C and F (see Fig. 4) over 10 years of operation.

for the field with multiple BHEs are still encouraging, as the absolute temperature change is also higher compared to the case with a single BHE. In addition to comparing the absolute values of the models, the evolution trend of the temperature change is also entirely consistent, which is an essential factor for optimization. The results confirm that the proposed restructured MFLS formulation can be adopted as a sound proxy for integration into a combined simulation-optimization-calibration framework for this BHEs configuration and the GWF patterns.

3.3. Optimal load balancing

In this section, the results of the proposed optimal load pattern for the case with ten BHEs assuming GWF pattern C are presented. The superiority of the proposed adaptive method compared to the single-step optimization approach for three selected time steps is shown in Fig. 7. The size of the circles depicts the relative load distribution among the BHEs in the field and the red circles show the position of the BHEs that cause the maximum temperature change. The advantage of the proposed method lies not only in the lower maximum temperature change, but also in the repositioning of the critical BHEs, which affects the location of the highest temperature change. Fig. 7 shows a modest improvement

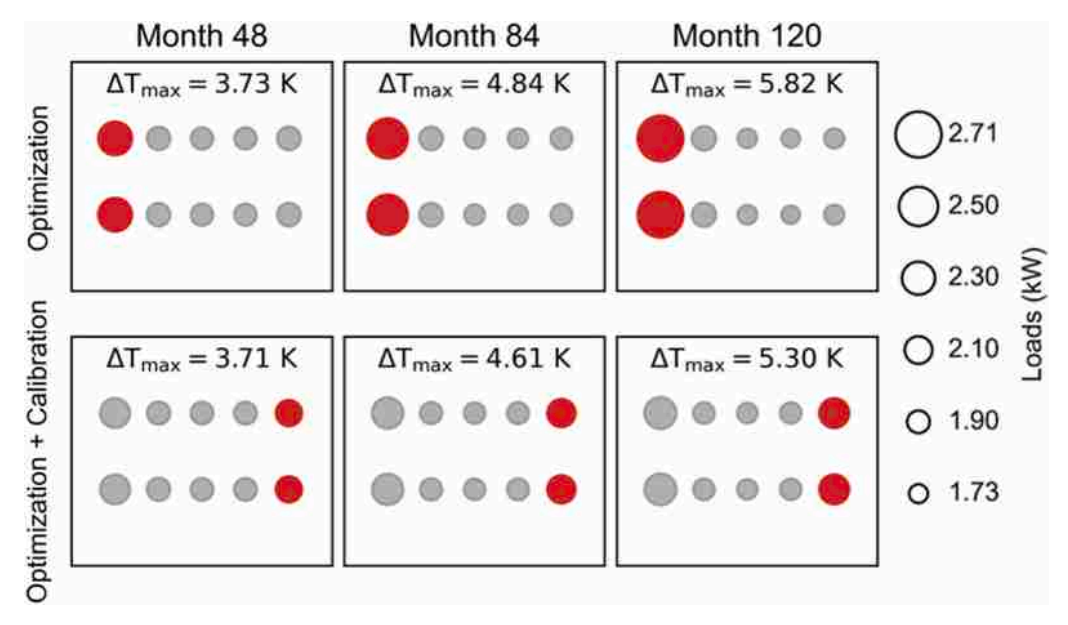


Fig. 7. Optimal load patterns at three time steps for the BHE field using the single-step optimization (top row) and the adaptive technique (bottom row). The size of the circles indicates the assigned load on each BHE and the red circle shows the BHE with the highest temperature change. The empty circles in the legend represent the relationship between heat extraction and the size of the circles.

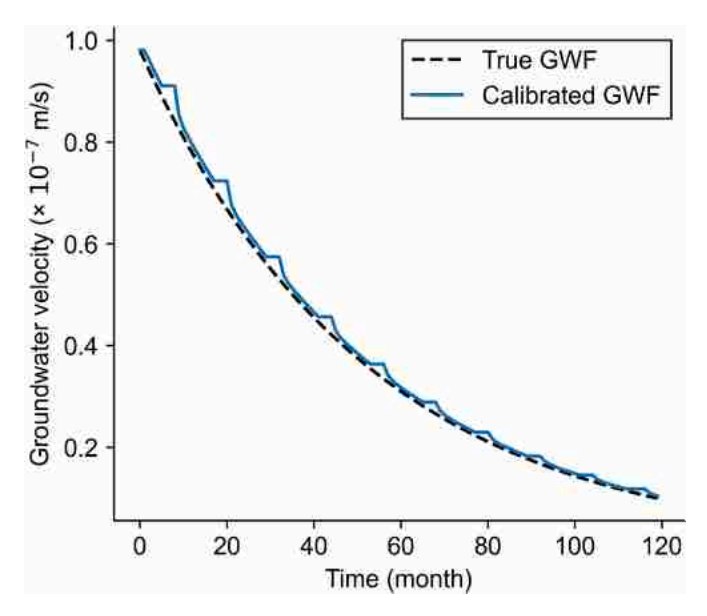


Fig. 8. Comparison of the monthly calibrated groundwater flow velocity values obtained by adaptive optimization (blue line) with the true pattern (dashed line).

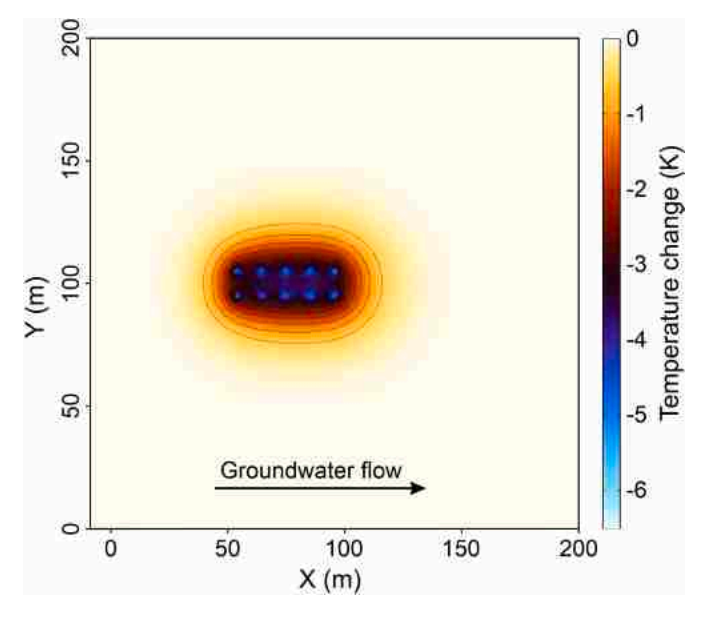


Fig. 9. Distribution of the resulting heat plume at a depth of 50 m after 10 years of operation in the case with simulation-optimization-calibration.

manifested in a 10 % reduction in the imposed temperature change, but it should be emphasized that both scenarios are subject to optimization, and this slight improvement highlights the role of model parameter estimation through the adaptive optimization strategy. It is also important to recognize that this discrepancy increases with longer operating time. The lack of calibration functionality in the initial case by the single-step optimization, which assumes a steady and constant GWF over the operating time, leads to a misinterpretation of the critical BHEs. Essentially, the results highlight that the use of a data assimilation strategy favors a more even load distribution within the BHE field and mitigates the impact of GWF magnitude on the upstream BHEs.

The calibrated GWF values compared to the real trend are shown in Fig. 8. One interesting aspect is that, for calibration, the highest deviations occur in the summer months. This is evident as stagnation is

attributed to the absence of any heating demand in the field. Thus, no new insights into the thermal conditions of the ground can be gained, which delays the learning process of the calibration, as no better values than in the previous months can be determined.

The thermal plume from the top view at a depth of 50 m is presented in Fig. 9. To avoid errors in reporting the absolute values of temperature change in this section, the optimal load balancing is executed using the proposed approach by the semi-analytical model due to its computational efficiency and flexibility enabling the combined optimization-calibration algorithm. The absolute temperature values are based on the implementation of resulting load patterns in a numerical model.

4. Conclusions and outlook

This study focuses on tuning the heating load of individual systems within a field operating with multiple borehole heat exchangers (BHEs). The proposed workflow involves a four-step recursive process: simulation, measurement, calibration, and optimization. What sets this work apart from previous studies is twofold: firstly, the functionality of the widely used moving finite line source (MFLS) analytical modeling tool through the rearrangement of its formulation is enhanced. This enhancement allows us to account for transient groundwater flow (GWF), thereby accommodating more realistic and complex subsurface conditions. It should be recalled that although the numerical model is more reliable, due to the iterative characteristic of the proposed methodology, the integration of the numerical model in the iterative simulation-optimization procedure is not computationally comparable. Secondly, the optimization process is more informative as it includes a parameter estimation in each time step. To validate the proposed formulation, numerical modeling of two case studies with varying GWF velocity patterns as a benchmark study is conducted. Then, the modified MFLS model is employed as the predictive tool for optimization. By solving a least square problem based on monthly measurements and simulations, the GWF velocity for the subsequent month is calibrated and updated optimal load patterns for the upcoming months are proposed. The result of the optimization for the case study with multiple BHEs indicates that the potential of the new workflow is to provide more insightful optimal load patterns that can be continuously modified. Through this modification, the imposed undesired thermal anomalies in the subsurface will be minimized. The main target of this workflow is to improve the sustainability and durability of closed-loop geothermal systems by addressing environmental concerns as well as making them economically viable. For future studies, it is proposed to integrate more robust simulation tools that can handle additional subsurface complexities, such as heterogeneity. Additionally, developing efficient proxy models to represent the subsurface complexity in a computationally feasible manner is recommended. Furthermore, using intelligent learning techniques for parameter estimation can have the potential to further enhance the efficiency of the calibration process.

Data availability

The associated data and codes for this study are available from the corresponding author upon request.

CRediT authorship contribution statement

Hesam Soltan Mohammadi: Conceptualization, Data curation, Formal analysis, Investigation, Methodology, Software, Validation, Visualization, Writing – original draft, Writing – review & editing. Lisa Maria Ringel: Conceptualization, Formal analysis, Investigation, Methodology, Validation, Writing – review & editing. Christoph Bott: Investigation, Validation, Visualization, Writing – review & editing. Peter Bayer: Conceptualization, Funding acquisition, Methodology, Resources, Project administration, Supervision, Writing – review & editing.

Declaration of competing interest

The authors declare that they have no known competing financial interests or personal relationships that could have appeared to influence the work reported in this paper.

Acknowledgments

This work was supported by the German Research Foundation (DFG) based on grant number BA2850/7-1, and by the Federal Ministry for Economic Affairs and Climate Action of Germany (BMWK) based on

grant number 03EE4039A, within the GEOTHERMICA project RECOIN (ID: 455). The authors thank Ryan Pearson, Wiebke Lehmann, and Lukas Römhild for proofreading, and Hannes Hemmerle for his help with the initial design of the graphical abstract. The authors also appreciate helpful and constructive comments from three anonymous reviewers.

References

- S.A. Benz, K. Menberg, P. Bayer, B.L. Kurylyk, Shallow subsurface heat recycling is a sustainable global space heating alternative, Nat. Commun. 13 (2022) 3962.
- [2] F. Stauffer, P. Bayer, P. Blum, N.M. Giraldo, W. Kinzelbach, Thermal Use of Shallow Groundwater, CRC Press, 2013.
- [3] S. Gehlin, Thermal Response Test: Method Development and Evaluation, 2002.
- [4] J.D. Spitler, S.E.A. Gehlin, Thermal response testing for ground source heat pump systems - an historical review, Renew. Sustain. Energy Rev. 50 (2015) 1125–1137, https://doi.org/10.1016/i.rser.2015.05.061.
- [5] M. Yoshioka, G. Shrestha, A. Widiatmojo, Y. Uchida, Seasonal changes in thermal process based on thermal response test of borehole heat exchanger, Geothermics 102 (2022) 102390, https://doi.org/10.1016/j.geothermics.2022.102390.
- [6] M. Noethen, H. Hemmerle, P. Bayer, Sources, intensities, and implications of subsurface warming in times of climate change, Crit. Rev. Environ. Sci. Technol. 53 (2023) 700–722.
- [7] V. Wagner, P. Bayer, M. Kübert, P. Blum, Numerical sensitivity study of thermal response tests, Renew. Energy 41 (2012) 245–253, https://doi.org/10.1016/j. renene.2011.11.001.
- [8] C.K. Lee, Effects of multiple ground layers on thermal response test analysis and ground-source heat pump simulation, Appl. Energy 88 (2011) 4405–4410, https:// doi.org/10.1016/j.apenergy.2011.05.023.
- [9] C. Zhang, J. Lu, X. Wang, H. Xu, S. Sun, Effect of geological stratification on estimated accuracy of ground thermal parameters in thermal response test, Renew. Energy 186 (2022) 585–595, https://doi.org/10.1016/j.renene.2022.01.024.
- [10] E. Heim, M. Laska, R. Becker, N. Klitzsch, Estimating the subsurface thermal conductivity and its uncertainty for shallow geothermal energy use—a workflow and geoportal based on publicly available data, Energies 15 (2022) 3687.
- [11] S. Robert, P. Pasquier, A. Nguyen, Impact of layered heterogeneity on thermal response test interpretation performed on a standing column well operated without bleed, Geothermics 101 (2022) 102353.
- [12] J. Luo, J. Tuo, W. Huang, Y.Q. Zhu, Y.Y. Jiao, W. Xiang, J. Rohn, Influence of groundwater levels on effective thermal conductivity of the ground and heat transfer rate of borehole heat exchangers, Appl. Therm. Eng. 128 (2018) 508–516, https://doi.org/10.1016/j.applthermaleng.2017.08.148.
- [13] B. Zhang, K. Gu, P. Bayer, H. Qi, B. Shi, B. Wang, Y. Jiang, Q. Zhou, Estimation of groundwater flow rate by an actively heated fiber optics based thermal response test in a grouted borehole, Water Resour. Res. 59 (2023) e2022WR032672.
- [14] A. Albers, H. Steger, R. Zorn, P. Blum, Evaluating an enhanced thermal response test (ETRT) with high groundwater flow, Geoth. Energy 12 (2024) 1–22, https://doi.org/10.1186/s40517-023-00278-y.
- [15] D. Banks, A review of the importance of regional groundwater advection for ground heat exchange, Environ. Earth Sci. 73 (2015) 2555–2565, https://doi.org/ 10.1077/e14655.014.2377.
- [16] Z. Zhao, Y.F. Lin, A. Stumpf, X. Wang, Assessing impacts of groundwater on geothermal heat exchangers: a review of methodology and modeling, Renew. Energy 190 (2022) 121–147, https://doi.org/10.1016/j.renene.2022.03.089.
- [17] J. Ma, Q. Jiang, Q. Zhang, Y. Xie, Y. Wang, F. Yi, Effect of groundwater forced seepage on heat transfer characteristics of borehole heat exchangers, Geoth. Energy 9 (2021) 1–23, https://doi.org/10.1186/s40517-021-00192-1.
- [18] D. Moreira, J. Macias, R. Hidalgo-Leon, F.X. Jervis, G. Soriano, Perfomance of a borehole heat exchanger: the influence of thermal properties estimation under tidal fluctuation, Eng. Sci. Technol. an Int. J. 30 (2022) 101057, https://doi.org/ 10.1016/j.jestch.2021.09.003.
- [19] Z. He, N. Zhou, C. Guo, J. Liu, Study on configurational operation strategy of ground heat exchangers under the effect of groundwater flow, Therm. Sci. Eng. Prog. 47 (2024) 102302, https://doi.org/10.1016/j.tsep.2023.102302.
- [20] F. Deng, W. Li, P. Pei, L. Wang, Y. Ren, Study on design and calculation method of borehole heat exchangers based on seasonal patterns of groundwater, Renew. Energy 220 (2024) 119711, https://doi.org/10.1016/j.renene.2023.119711.
- [21] W. Li, X. Li, Y. Peng, Y. Wang, J. Tu, Experimental and numerical studies on the thermal performance of ground heat exchangers in a layered subsurface with groundwater, Renew. Energy 147 (2020) 620–629, https://doi.org/10.1016/j. renene.2019.09.008.
- [22] VDI, Thermal Use of the Underground. Part 2: Geothermal Heat Pump Systems: VDI 4640, Düsseldorf, VDI-Verlag, Düsseldorf, 2001, p. 43.
- [23] P. Blum, K. Menberg, F. Koch, S.A. Benz, C. Tissen, H. Hemmerle, P. Bayer, Is thermal use of groundwater a pollution? J. Contam. Hydrol. 239 (2021) 103791 https://doi.org/10.1016/j.jconhyd.2021.103791.
- [24] M. Beck, J. Hecht-Méndez, M. De Paly, P. Bayer, P. Blum, A. Zell, Optimization of the energy extraction of a shallow geothermal system, in: 2010 IEEE World Congr. Comput. Intell. WCCI 2010 - 2010 IEEE Congr. Evol. Comput. CEC 2010, 2010, https://doi.org/10.1109/CEC.2010.5585921.
- [25] M. Beck, P. Bayer, M. de Paly, J. Hecht-Méndez, A. Zell, Geometric arrangement and operation mode adjustment in low-enthalpy geothermal borehole fields for heating, Energy 49 (2013) 434–443, https://doi.org/10.1016/j. energy.2012.10.060.

- [26] P. Bayer, M. de Paly, M. Beck, Strategic optimization of borehole heat exchanger field for seasonal geothermal heating and cooling, Appl. Energy 136 (2014) 445–453, https://doi.org/10.1016/j.apenergy.2014.09.029.
- [27] J. Hecht-Méndez, M. De Paly, M. Beck, P. Bayer, Optimization of energy extraction for vertical closed-loop geothermal systems considering groundwater flow, Energy Convers. Manag. 66 (2013) 1–10, https://doi.org/10.1016/j. enconman.2012.09.019.
- [28] N. Egidi, J. Giacomini, P. Maponi, Inverse heat conduction to model and optimise a geothermal field, J. Comput. Appl. Math. 423 (2023) 114957, https://doi.org/ 10.1016/j.cam.2022.114957.
- [29] A. Noel, M. Cimmino, Development of a Topology Optimization Method for the Design of Ground Heat Exchangers, 2022.
- [30] J.D. Spitler, T. West, X. Liu, Ground Heat Exchanger Design Tool with Rowwise Placement of Boreholes, 2022.
- [31] J.D. Spitler, J.C. Cook, X. Liu, A preliminary investigation on the cost reduction potential of optimizing bore fields for commercial ground source heat pump systems, 45th work. Geotherm. Reserv, Engage (2020) 1–13.
- [32] M. Cimmino, Pe Michel Bernier PhD, Effects of unequal borehole spacing on the required borehole length, Build. Eng. 120 (2014) 158.
- [33] H. Javadi, S.S. Mousavi Ajarostaghi, M.A. Rosen, M. Pourfallah, Performance of ground heat exchangers: a comprehensive review of recent advances, Energy 178 (2019) 207–233, https://doi.org/10.1016/j.energy.2019.04.094.
- [34] E. Heim, P. Stoffel, S. Düber, D. Knapp, A. Kümpel, D. Müller, N. Klitzsch, Comparison of simulation tools for optimizing borehole heat exchanger field operation, Geothermal Energy 24 (2024) 12–24, https://doi.org/10.1186/s40517-024.00303.8
- [35] P. Stoffel, A. Kümpel, D. Müller, Cloud-based optimal control of individual borehole heat exchangers in a geothermal field, J. Therm. Sci. 31 (2022) 1253–1265, https://doi.org/10.1007/s11630-022-1639-0.
- [36] A. Kümpel, P. Stoffel, D. Müller, Development of a long-term operational optimization model for a building energy system supplied by a geothermal field, J. Therm. Sci. 31 (2022) 1293–1301, https://doi.org/10.1007/s11630-022-1616-7.
- [37] P. Stoffel, L. Maier, A. Kümpel, T. Schreiber, D. Müller, Evaluation of advanced control strategies for building energy systems, Energy Build. 280 (2023) 112709, https://doi.org/10.1016/j.enbuild.2022.112709.
- [38] F. De Ridder, M. Diehl, G. Mulder, J. Desmedt, J. Van Bael, An optimal control algorithm for borehole thermal energy storage systems, Energy Build. 43 (2011) 2918–2925, https://doi.org/10.1016/j.enbuild.2011.07.015.
- [39] E. Atam, D. Patteeuw, S.P. Antonov, L. Helsen, Optimal control approaches for analysis of energy use minimization of hybrid ground-coupled heat pump systems, IEEE Trans. Control Syst. Technol. 24 (2016) 525–540, https://doi.org/10.1109/ TCST.2015.2445851.

- [40] W. Gang, J. Wang, S. Wang, Performance analysis of hybrid ground source heat pump systems based on ANN predictive control, Appl. Energy 136 (2014) 1138–1144, https://doi.org/10.1016/j.apenergy.2014.04.005.
- [41] S. Ikeda, W. Choi, R. Ooka, Optimization method for multiple heat source operation including ground source heat pump considering dynamic variation in ground temperature, Appl. Energy 193 (2017) 466–478, https://doi.org/10.1016/ i.apenergy.2017.02.047.
- [42] H. Soltan Mohammadi, L.M. Ringel, P. Bayer, Sequential simulation-optimization of a borehole heat exchanger field considering variability in heating demand and subsurface thermal responses, Copernicus Meetings EGU23-3243 (2023), https:// doi.org/10.5194/egusphere-egu23-3243.
- [43] H. Soltan Mohammadi, L.M. Ringel, M. de Paly, P. Bayer, Sequential long-term optimization of shallow geothermal systems under descriptive uncertainty and dynamic variation of heating demand, Geothermics 121 (2024) 103021, https:// doi.org/10.1016/j.geothermics.2024.103021.
- [44] H.Y. Zeng, N.R. Diao, Z.H. Fang, A finite line-source model for boreholes in geothermal heat exchangers, Heat Tran. Asian Res. 31 (2002) 558–567, https://doi.org/10.1002/hti.10057.
- [45] N. Molina-Giraldo, P. Blum, K. Zhu, P. Bayer, Z. Fang, A moving finite line source model to simulate borehole heat exchangers with groundwater advection, Int. J. Therm. Sci. 50 (2011) 2506–2513, https://doi.org/10.1016/j. iithermalsci.2011.06.012.
- [46] M. De Paly, J. Hecht-Méndez, M. Beck, P. Blum, A. Zell, P. Bayer, Optimization of energy extraction for closed shallow geothermal systems using linear programming, Geothermics 43 (2012) 57–65, https://doi.org/10.1016/j. geothermics.2012.03.001.
- [47] S. Erol, M.A. Hashemi, B. François, Analytical solution of discontinuous heat extraction for sustainability and recovery aspects of borehole heat exchangers, Int. J. Therm. Sci. 88 (2015) 47–58, https://doi.org/10.1016/j. iithermalsci.2014.09.007.
- [48] S. Erol, B. François, Multilayer analytical model for vertical ground heat exchanger with groundwater flow, Geothermics 71 (2018) 294–305, https://doi.org/ 10.1016/j.geothermics.2017.09.008.
- [49] M. Fossa, The temperature penalty approach to the design of borehole heat exchangers for heat pump applications, Energy Build. 43 (2011) 1473–1479, https://doi.org/10.1016/j.enbuild.2011.02.020.
- [50] P. Pasquier, L. Lamarche, Analytic expressions for the moving infinite line source model, Geothermics 103 (2022) 102413, https://doi.org/10.1016/j. geothermics.2022.102413.
- [51] R.H. Byrd, J.C. Gilbert, J. Nocedal, A trust region method based on interior point techniques for nonlinear programming. Math. Program. 89 (2000) 149–185.
- [52] M. Cimmino, The effects of borehole thermal resistances and fluid flow rate on the g-functions of geothermal bore fields, Int. J. Heat Mass Tran. 91 (2015) 1119–1127, https://doi.org/10.1016/j.ijheatmasstransfer.2015.08.041.